Biomed Microdevices (2009) 11:579–583
DOI 10.1007/s10544-008-9267-3

Hybridization of localized surface plasmon resonance-based Au–Ag nanoparticles

Shaoli Zhu · Yongqi Fu

Published online: 16 December 2008

Abstract The hybrid Au–Ag triangular nanoparticles were proposed for the purpose of biosensing. To construct the nanoparticles, an Au thin film was deposited on top of the Ag nanoparticles supported with glass substrate. The hybrid nanoparticles can prevent oxidation of the pure Ag nanoparticles due to the Au protective layer caped on the Ag nanoparticles. The hybrid nanoparticles were designed using finite-difference and time-domain algorithm. Extinction spectra of the hybrid nanoparticles excited by visible light beam with plane wave were calculated, and the corresponding electric fields at peak position of the extinction spectra were expressed also. It is clear that the hybrid nanoparticles can excite the localized surface plasmon resonance wave which can be used to detect biomolecules. As an application example, we presented relevant detection results by means of using protein A to covalently link surface of the hybrid nanoparticles. Refractive index sensitivity of the hybrid nanoparticles was derived through both computational numerical calculation and experimental detection. Both the calculated and the experimental extinction spectra show that the hybrid Au–Ag nanoparticles are useful for detecting the biomolecules.

Keywords Hybrid Au–Ag nanoparticles · Nano-biosensor · LSPR · Spectroscopy

S. Zhu (✉)
Photonics Centre, School of Electronic and Electrical Engineering, Nanyang Technological University,
50 Nanyang Avenue,
Singapore 639798, Singapore
e-mail: slzhu@ntu.edu.sg

Y. Fu
School of Physical Electronics,
University of Electronic Science and Technology of China,
Chengdu 610054, Sichuan Province, People's Republic of China

1 Introduction

Localized surface plasmon resonance (LSPR) nanobiosensors are of great interest in various applications such as environmental protection, (Ji et al. 2004; Ligler et al. 2003) bionanotechnology, (Kohls and Scheper 2000) and food safety (Ligler et al. 2003, Wiskur and Anslyn 2001). Recently, several research groups have begun to explore alternative strategies for development of the optical biosensors and chemosensors (Malinsky et al. 2001) working on the basis of the extraordinary optical properties of noble metal nanoparticles. They possesses a strong ultraviolet-visible absorption band that is not presented in the spectrum of the bulk metal. (Haynes and Van Duyne 2001) This absorption occurs when the incident photon frequency is resonant with the collective oscillation of the conduction electrons and is know as LSPR. It is well established that the nanoscale chemosensors and biosensors can be realized through shifts in the LSPR-based resonance peak transmission λ_{max} of extinction spectrum of the silver nanoparticles. (Malinsky et al. 2001) These wavelength shifts are caused by adsorbate-induced local refractive index variations in competition with charge-transfer interactions on the nanoparticles surface. In this research domain, representative works have been performed by Northwestern University. (Haes and Van Duyne 2002; Haes and Van Duyne 2003; Riboh et al. 2003; Haes et al. 2004, Yonzon et al. 2004) One of their research subjects focused on the measurement of binding signal between antigen and antibody with the Ag triangular nanoparticles. However, there are high requirements for researching novel LSPR-based hybrid metal nanostructures. In this paper, considering microfabrication capability and the application request for the nanoparticles of the biochemistry chip, a hybrid Au–Ag triangular nanoparticles is introduced for achieving higher sensitivity. Using finite-difference and time-domain

(FDTD) algorithm, we designed the extinction spectra and the corresponding electric fields at the extinction spectra peak position of the hybrid nanoparticles. We developed an extended nanosphere lithography (NSL) method to fabricate the hybrid Au–Ag triangular nanoparticles array with in-plane widths of ~100 nm, out-of-plane heights of Ag ~50 nm, upper Au thickness of ~5 nm, and 400 nm period of the particles array.

2 Hybrid Au–Ag nanoparticles

The hybrid Au–Ag triangular nanoparticles were proposed as a sensitive cell of the LSPR-based nano-biosensor. Using the FDTD algorithm, we designed and calculated the extinction spectra as well as the corresponding electric field of the hybrid nanoparticles array. A cross-section of a single particle labeling the materials of the substrate and particle as well as their thicknesses is shown in Fig. 1. Glass substrate is considered in the simulation while we created three-dimensional model. This model is almost close to the actual experimental sample. To simulate the Protein A binding to surface of the gold nanoparticles, we change the refractive index around the gold nanoparticles including the effect of the glass substrate only. A global index change was not assumed when protein A is bound.

Out-of plane height of the silver nanoparticles is 50 nm and the upper Au nanoparticles are 5 nm in height, and the in plane widths of each nanoparticles is 100 nm. The period of the nanoparticle array is 400 nm and wavelength of the incidence white light source is ranging from 400 nm to 700 nm. The incidence light beam is projected in perpendicular to the substrate. In order to investigate the transmission property of different refractive index of the mediums surrounding this hybrid nanoparticles, we selected the mediums of air (n_1=1.0) and Protein A (Protein A: PBS (0.01 M, pH 7.4)=1:100, n_2= 1.3352) surrounding the nanoparticles. When the refractive indexes of the surrounding mediums are 1.0 and 1.3352, the computational results using FDTD method are shown in Fig. 2. From the result, we can obtain sensitivity of the hybrid Au–Ag triangular nanoparticles as $S = \frac{\lambda_{\max 1} - \lambda_{\max 2}}{n_2 - n_1} = \frac{551.638 - 484.513}{1.3352 - 1.0} = 200$ nm/RIU. Thus it is reasonable to believe that the hybrid nanoparticles can realize a higher sensitivity detection of biomolecules. The protein layer is likely to be thinner than the E-field evanescent wave decay. But it is the air around the gold nanoparticles before and after the protein A binding to the surface of the gold nanoparticles, and hence the change of the extinction spectra is caused by the binding of the protein A only. Therefore, it can not reduce the experimental sensitivity.

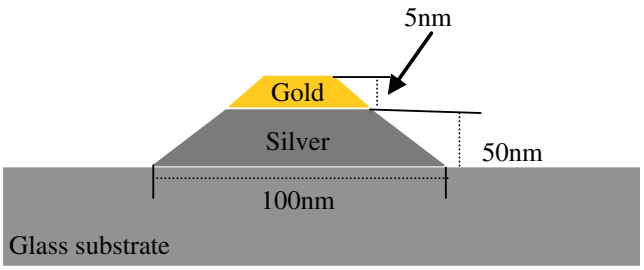

Fig. 1 Cross-section of a single hybrid Au–Ag triangular nanoparticles

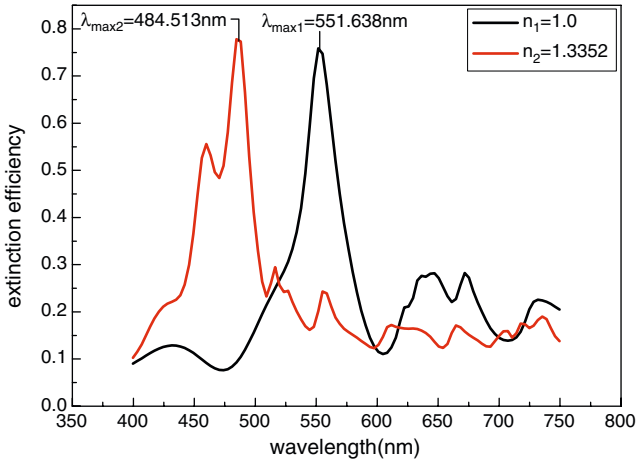

Fig. 2 FDTD solution calculated result when the refractive index medium surrounding this hybrid nanoparticles are 1.0 and 1.3352, respectively

In addition, we calculated the electric fields when the incident light wavelength is equal to the LSPR wavelength λ_{SPP}. The electric fields can be expressed as $\mathbf{E}^2 = \mathbf{E}_x^2 + \mathbf{E}_y^2 + \mathbf{E}_z^2$. Using the FDTD algorithm, we obtained the electric field $\mathbf{E}$ for the incident light wavelength λ_{in}= 551.638 nm (refractive index of the medium surrounding this hybrid nanoparticles is n_d=1.0). The electric field is also calculated for λ_{in}=484.513 nm (refractive index of the medium surrounding this hybrid nanoparticles is n_d= 1.3352). Figure 3 shows the calculated results of the electric field in the case of $\lambda_{in}=\lambda_{SPP}$. It can be seen from Fig. 3 that the total electric field $\mathbf{E}$ from Au surface of 5 nm in thickness changed tremendously as well when the refractive index of the medium surrounding the hybrid nanoparticles is n_d=1.0. These results indicated that the hybrid Au–Ag triangular nanoparticles can function as a platform for detecting the biomolecules such as Protein A.

3 Experimental setup

3.1 Chemical materials

Our experiments were carried out using Protein A which was from Sigma-Aldrich; and phosphate buffer solution (PBS, 0.01 M, pH 7.4)) from Jinshan Chemical Analyte

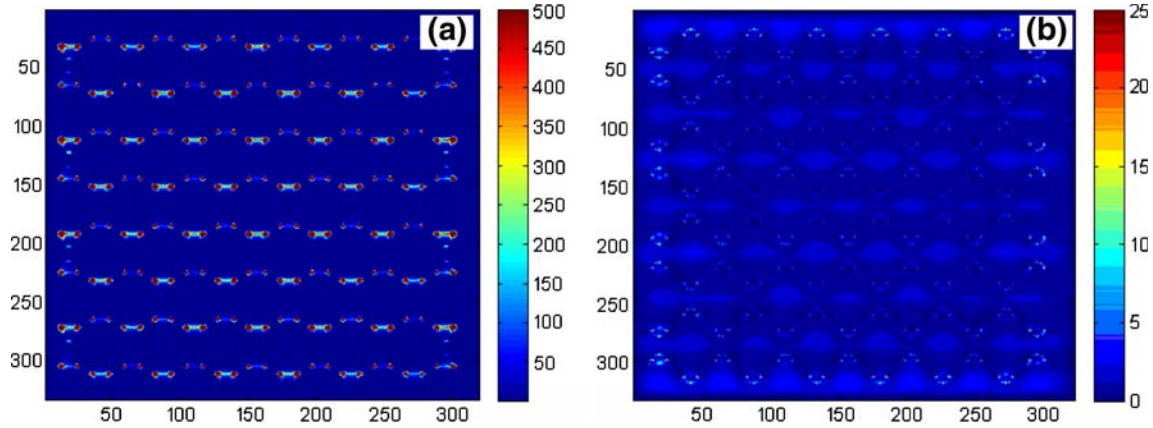

Fig. 3 FDTD solution calculated electric field result when the incidence light wavelength is equal to the LSPR wavelength. (**a**) Total electric field $\mathbf{E}^2 = \mathbf{E}_x^2 + \mathbf{E}_y^2 + \mathbf{E}_z^2$ from Au surface 5 nm; n=1.0, $\lambda_{in}=\lambda_{max}$=551.638 nm; (**b**) Total electric field $\mathbf{E}^2 = \mathbf{E}_x^2 + \mathbf{E}_y^2 + \mathbf{E}_z^2$ from Au surface 5 nm; n=1.3352, $\lambda_{in}=\lambda_{max}$=484.513 nm

Pte. Ltd. The buffer used in the experiments was prepared using double glass-distilled water.

3.2 Integrated LSPR sensor

The integrated LSPR sensor used in this work is our home-built system. The peak wavelengths of the LSPR extinction spectra (λ_{max}) excited by the hybrid Au–Ag triangular nanoparticles were measured and recorded using UV-Visible spectroscopy. Practical measurements of the UV-Visible extinction spectra were achieved using a fiber-coupled spectrometer (Ocean Optics USB4000) and a CCD detector. The experimental setup and subsequent spectrum measurements were conducted using a conventional optical system with a non-polarized light beam working in the far-field region. The detection area of the bio-sensor was approximately 2×2 mm. All the extinction spectra were directly derived using professional software (from Ocean Optics Corp.) that was packaged together with the corresponding hardwares. Figure 4 depicts a schematic diagram of the light path and measurement set-up of Optical fiber (Ocean Optics USB4000) coupled spectrometric system. A shift towards longer wavelengths is referred to as a red-shift, and is denoted as (+), while a shift towards shorter wavelengths is referred to as a blue-shift, and is denoted as (−). Protein A has a specific binding to gold particles. Fabrication section of

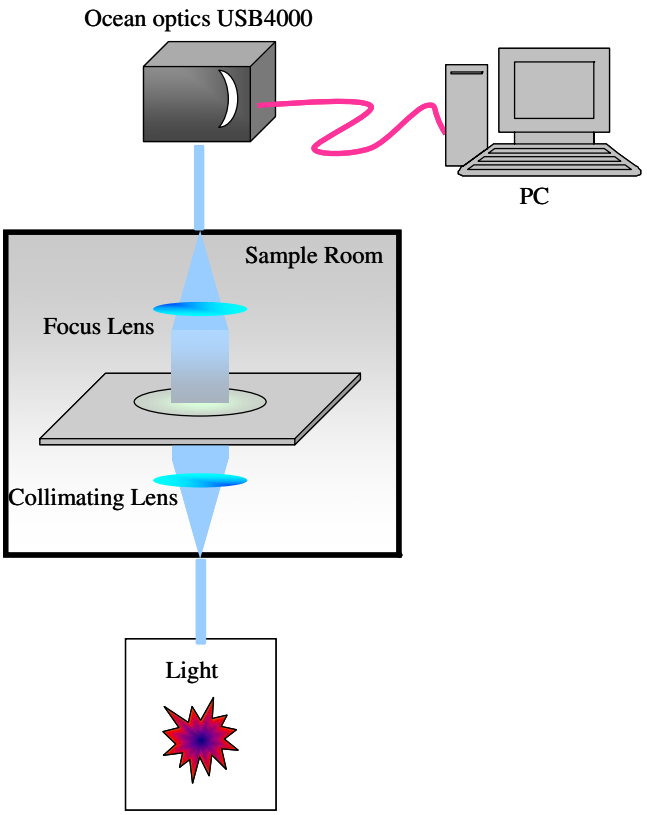

Fig. 4 A schematic diagram of the light path and measurement set-up of Optical fiber (Ocean Optics USB4000) coupled spectrometric system

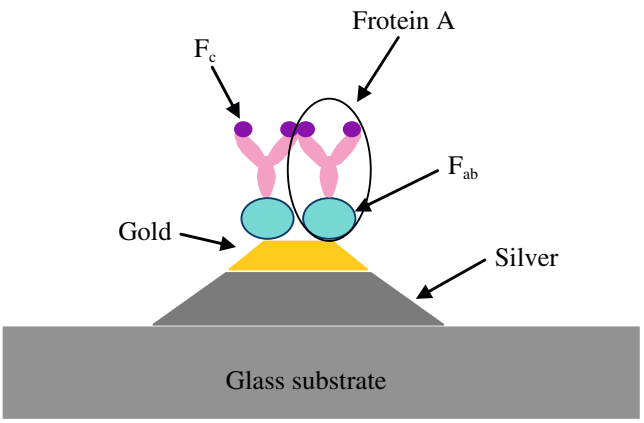

Fig. 5. Schematic diagram of the Fc directed method binding to the surface of gold nanoparticles

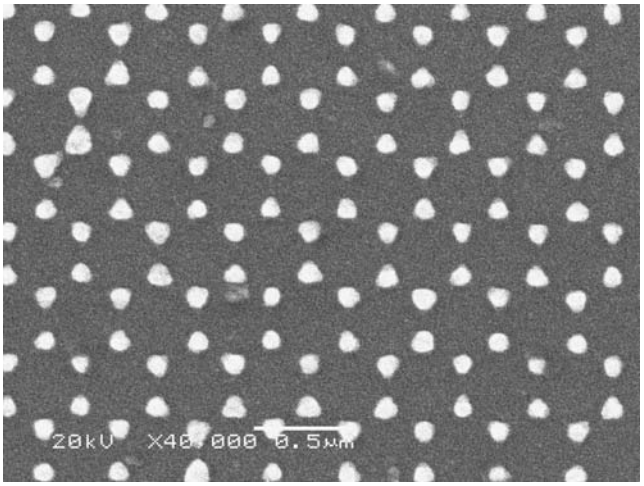

Fig. 6 SEM image of topography of the triangular hybrid Au–Ag nanoparticles fabricated by NSL

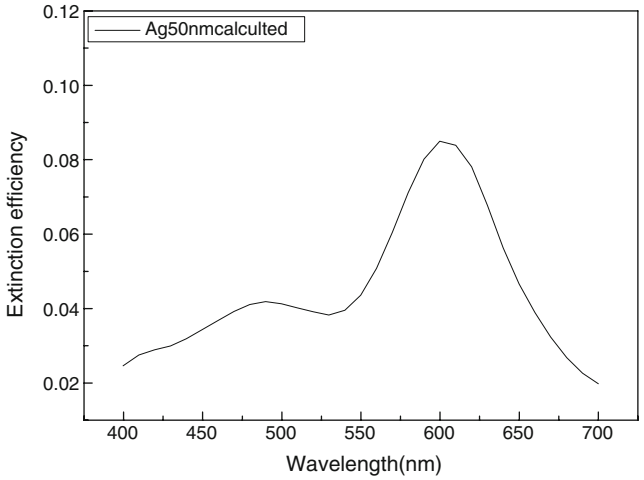

Fig. 8 Simulation result of extinction efficiency for silver-only nanoparticles All the parameters are same as the hybrid Au–Ag nanoparticles. Out-of plane height of the silver nanoparticles is 50 nm, and the in plane widths of each nanoparticles is 100 nm. The period of the nanoparticle array is 400 nm and wavelength of the incidence white light source is ranging from 400 nm to 700 nm. The incidence light beam is projected in perpendicular to the substratesimulation

protein A illustrates a specific biding to the surface of the gold nanopartices and the other section of Fc can bind to the other protein if it is necessary, as shown in Fig. 5.

4 Fabrication of the LSPR-based nano-biosensor

A NSL technique (Haes and Van Duyne 2002) was employed to create the surface-confined hybrid Au–Ag triangular nanoparticles supported on a glass substrate (see Fig. 6). NSL process begins from the self-assembly of size-monodisperse nanospheres into a two-dimensional (2D) colloidal crystal. As the solvent of the nanosphere solution evaporates, capillary forces draw the nanospheres together, thereby crystallizing them into a hexagonally close-packed pattern on the substrate. Following self-assembly of the nanosphere mask, both silver and gold thin films are deposited onto the nanosphere-coated substrate, respectively. After the films deposition, the nanosphere mask is removed via sonication in ethanol resulting in surface-confined nanoparticles with triangular footprints. The nanoparticles have out-of plane heights of silver nanoparticles ~50 nm and the upper gold nanoparticles ~5 nm in

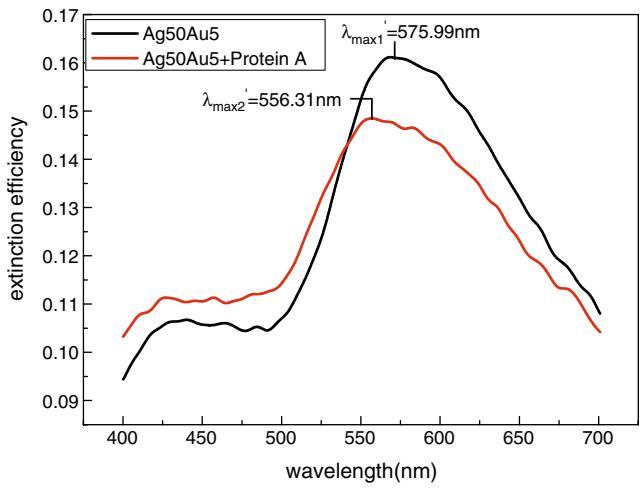

Fig. 7 Measured spectra for both pure hybrid Au–Ag (thickness of the Ag and Au is 50 nm and 5 nm, respectively) nanoparticles array and binding with protein A

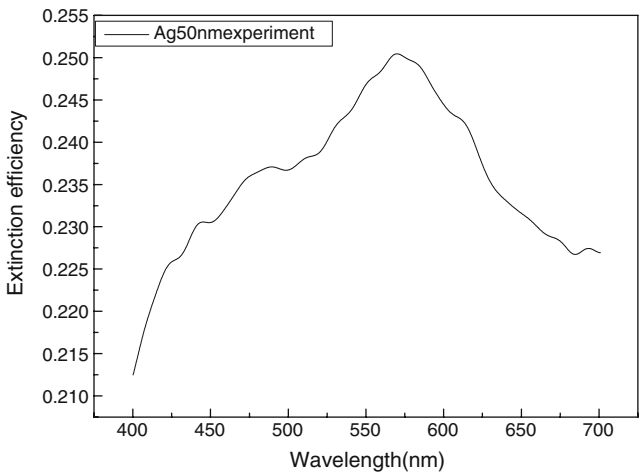

Fig. 9. Experiment result of extinction efficiency for silver-only nanoparticles

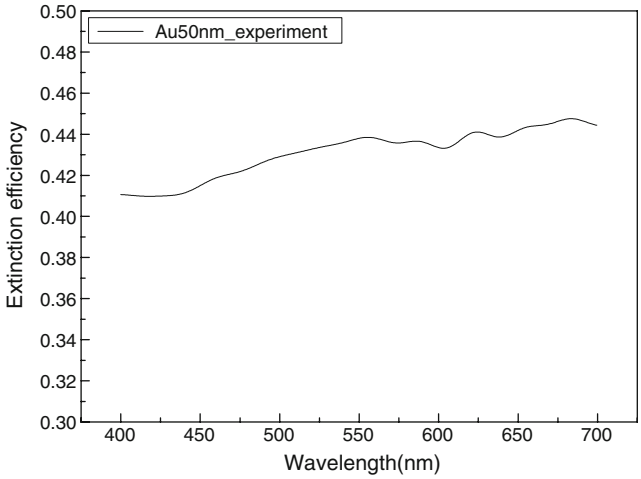

Fig. 10 Experiment result of extinction efficiency for gold-only nanoparticles

thickness, and ~100 nm in plane widths of each nanostructure and ~400 nm in period of the nanoparticle array as measured using JSM-5900 LA scanning electron microscope (SEM).

5 Results and discussion

The LSPR-based nano-biosensors are extremely sensitive to variation of effective refractive index (ERI) within a few hundred nanometers on gold surface. Capture of the target analyte (Protein A) by the specific reaction between the metal Au and the Protein A. Protein A bound to the sensing face changes the apparent RI due to solution displacement by the analytes of higher refractive index. To test the detection capability of the hybrid Au–Ag nano-biosensors, experiments were performed using solutions of Protein A in PBS buffer (1:100), and the refractive index of Protein A (1.3352) was detected by Abbe refractometer ZWA-J (temperature 20°C, $\Delta n=\pm 0.0002$). In this study, the LSPR spectra of the specific binding signal between the hybrid Au–Ag nano-biosensor and Protein A were monitored by the integrated LSPR sensor (see Fig. 7).

Resonant wavelength λ_{max} of the bare hybrid Au–Ag nanoparticles (see Fig. 7, black line) was measured to be 575.99 nm. Exposure to 1:100 Protein A resolution, resulted in $\lambda_{max}=556.31$ nm (see Fig. 7, red line), corresponding to a −19.68 nm shift. It should be noted that $\Delta\lambda_{max}=-19.68$ nm is smaller than the calculated result of the FDTD. It attributes the experimental defects caused by the NSL fabrication technique. Further study and modification will be performed in our next research project. All the extinction measurements were collected in atmosphere environment. It can be seen from Figs. 8 and 9 that FWHM of the extinction spectra of the hybrid Au–Ag nanoparticles is narrower than that of the pure silver nanoparticles. Thus we can draw a conclusion that the hybrid Au–Ag nanoparticles can improve the resolution of the nanobiosensor. From Fig. 10, it can be seen that the extinction spectra of the gold nanoparticles has no extinction peak. Hence the pure gold particles are not suitable to be used as the LSPR nanobiosensors. This is determined by the metal characters of the gold. These results demonstrate the practical benefit of the capping layer of gold to the silver. The difference between the simulation and experiment is caused by the error of the experiment, e.g., the NSL fabrication error and the measurement error.

6 Conclusions

We proposed a hybrid Au–Ag triangular nanoparticles array for the purpose of detection of a protein A. The hybrid Au–Ag particles can protect oxidation and sulfuration of the pure Ag particles from ambient environment. The typical protein can directly bind on the surface of Au film. Using our developed LSPR-based nano-biosensor with the hybrid Au–Ag nanoparticles, we can realize the refractive index sensitivity of 200 nm/RIU at atmosphere. The nano-biosensor demonstrates the potential applications in monitoring, detection and identification of biological agents, immunoassay as well as characterization of intermolecular interactions.

References

A.J. Haes, R.P. Van Duyne, J. Am. Chem. Soc. **124**, 10596–10604 (2002). doi:10.1021/ja020393x
A.J. Haes, R.P. Van Duyne, Laser Focus World **39**(5), 153–156 (2003)
A.J. Haes, S. Zou, G.C. Schatz, R.P. Van Duyne, J. Phys. Chem. B **108**, 109–116 (2004). doi:10.1021/jp0361327
C.L. Haynes, R.P. Van Duyne, J. Phys. Chem. B **105**, 5599–5611 (2001). doi:10.1021/jp010657m
J. Ji, J.A. Schanzle, M.B. Tabacco, Anal. Chem. **76**, 1411–1418 (2004). doi:10.1021/ac034914q
O. Kohls, T. Scheper, Sens. Actuators B Chem. **70**, 121–130 (2000). doi:10.1016/S0925-4005(00)00581-5
F.S. Ligler, C.R. Taitt, L.C. Shriver-Lake, K.E. Sapsford, Y. Shubin, J. P. Golden. Anal. Bioanal. Chem. **377**(3), 469–477 (2003). doi:10.1007/s00216-003-1992-0
M.D. Malinsky, K.L. Kelly, G.C. Schatz, R.P. Van Duyne, J. Am. Chem. Soc. **123**, 1471–1482 (2001). doi:10.1021/ja003312a
J.C. Riboh, A.J. Haes, A.D. McFarland, C. Ranjit, R.P. Van Duyne, J. Phys. Chem. B **107**, 1772–1780 (2003). doi:10.1021/jp022130v
S.L. Wiskur, E.V. Anslyn, J. Am. Chem. Soc. **123**(41), 10109–10110 (2001). doi:10.1021/ja011800s
C.R. Yonzon, E. Jeoung, S. Zou, G.C. Schatz, M. Mrksich, R.P. Van Duyne, J. Am. Chem. Soc. **126**, 12669–12676 (2004). doi:10.1021/ja047118q